Color Polymorphism: Understanding the Diverse Solid-State Packing and Color in Dimethyl-3,6-dichloro-2,5dihydroxyterephthalate

ARTICLE *in* CHEMISTRY - A EUROPEAN JOURNAL · MARCH 2014

Impact Factor: 5.73 · DOI: 10.1002/chem.201303322 · Source: PubMed

4 AUTHORS, INCLUDING:

A. Nijamudheen
University at Buffalo, The State University o…
24 PUBLICATIONS **173** CITATIONS
SEE PROFILE

Ayan Datta
Indian Association for the Cultivation of Sci…
94 PUBLICATIONS **1,474** CITATIONS
SEE PROFILE

ChemPubSoc Europe

DOI: 10.1002/chem.201303322

CHEMISTRY A European Journal Full Paper

Polymorphism

Color Polymorphism: Understanding the Diverse Solid-State Packing and Color in Dimethyl-3,6-dichloro-2,5-dihydroxyterephthalate

Saied Md. Pratik, Abdulrahiman Nijamudheen, Sumantra Bhattacharya, and Ayan Datta*[a]

Abstract: Dimethyl-3,6-dichloro-2,5-dihydroxyterephthalate (MCHT) is known to exist in three differently packed crystals having three different colors, namely yellow (Y), light yellow (LY), and white (W). Apart from the difference in their color, the molecules in the crystals also differ in their intramolecular O–H···O and O–H···Cl hydrogen bonds. Time-dependent DFT calculations reveal the role of the various types of hydrogen bonds in controlling the color of the polymorphs. Mechanistic pathways that lead to such transformations in the crystal are elucidated by solid-state dispersion-corrected DFT studies. Relative stabilities of the various polymorphs rationalize the experimentally observed transformations between them. Calculations reveal that the minimum-energy pathway for the conversion of the Y form to a W form is through stepwise disrotatory motion of the two –OH groups through a hybrid intermediate having one intramolecular O–H···O and one O–H···Cl bond. The LY form is shown to exist on the higher-energy pathway involving a concerted Y→W transformation.

Introduction

The chemistry of dynamically flexible molecules has gained importance in the last decade due to the possibility of designing molecular motors and rotors based on this principle.[1,2] The relatively easy rotation along single bonds and across weakly bound systems, such as hydrogen bonds[3] and salt bridges[4] leads to interesting conformational states for peptides[5] (folded and unfolded forms), polymers,[6] and self-assembled monolayers (SAMs).[7] The different states of conformationally active molecules have been probed by a variety of tools, such as UV/Vis spectroscopy, fluorescence resonance energy transfer, and second harmonic generation, and have been imaged by scanning tunneling microscopy techniques in which the molecules have been assembled over surfaces.

Apart from having intramolecular conformationally active states, flexible rotation along the single bonds leads to interesting diversity in their intermolecular packing. Odd–even oscillation in the melting points of hydrocarbons and packing efficiencies of SAMs have been understood based on the intramolecular conformations in the individual molecules that arrange differently among themselves.[8,9] Differences in packing of the same molecule lead to formation of several different crystalline phases called polymorphs. Although polymorphism is observed for even rigid molecules such as naphthalene and anthracene, it is much more commonplace for molecules with flexible side chains. Understanding of the processes involved in aggregation of molecules to form polymorphic crystals is being increasingly realized in the pharmaceutical industry and materials science.[10] In this context, a few polymorphs have been shown not only to have different molecular arrangements and consequent different lattice parameters but also to have different colors.

The most well-known example of color polymorphism is for 5-methyl-2-[(2-nitrophenyl)amino]-3-thiophenecarbonitrile, which is known to exist in seven polymorphs with still many phases yet to be determined.[11] Three of its polymorphs have three different colors, namely red, orange, and yellow, which has led to the crystals being popularly called ROY. Melting and eutectic melting data show that all the available seven polymorphic crystals are within approximately 1 kcal mol^{-1} of relative enthalpies of formation. The other well-characterized system that undergoes such color polymorphism is dimethyl-3,6-dichloro-2,5-dihydroxyterephthalate (MCHT). MCHT is known to exist in three different polymorphs having different colors, namely yellow (Y), light yellow (LY), and white (W) (see Figure 1), depending on the temperature of the reaction and the polarity of the solvents used during crystallization.[12] For the Y crystal, the crystal structure as well as Raman spectra show that the molecule is planar with the two hydroxyl groups interacting through intramolecular O–H···O hydrogen bonds with carboxymethyl groups.[13] For the LY form, the carboxymethyl groups are bent with respect to the benzene ring, which results in longer (hence weaker) O–H···O bonds. For the W form, the rupture of the O–H···O hydrogen bonds is complete, which results in 180° rotation of the hydroxyl groups to

[a] S. M. Pratik, A. Nijamudheen, S. Bhattacharya, Dr. A. Datta
Department of Spectroscopy
Indian Association for the Cultivation of Science
Jadavpur 700032, West Bengal (India)
E-mail: spad@iacs.res.in

Supporting information (Cartesian coordinates, energies, complete Gaussian 09 and Quantum Espresso reference) for this article is available on the WWW under http://dx.doi.org/10.1002/chem.201303322.

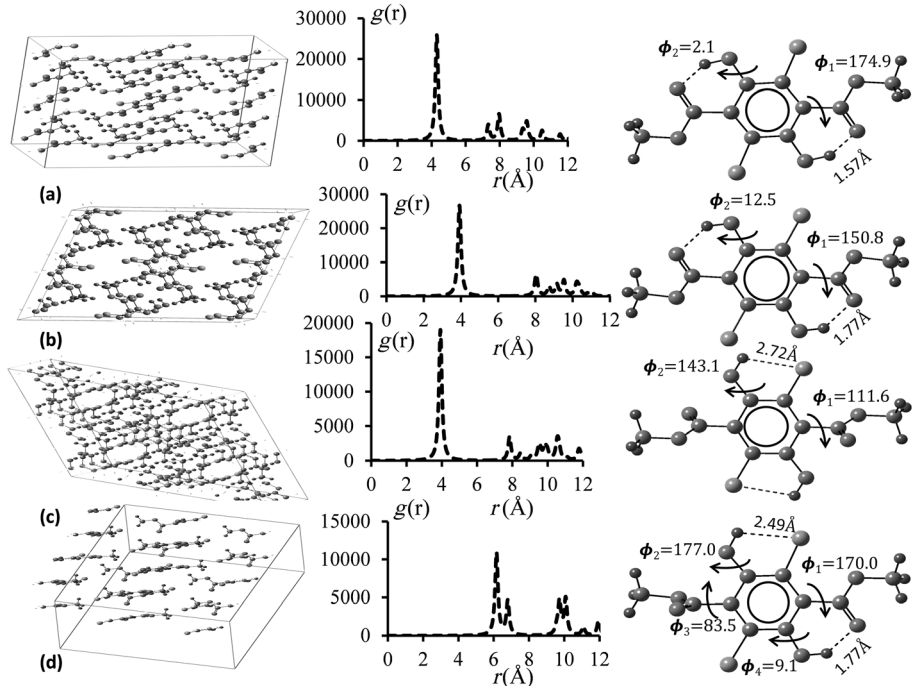

Figure 1. Optimized crystal structures for a) yellow, b) light yellow, c) white, and d) hybrid crystals of dimethyl-3,6-dichloro-2,5-dihydroxyterephthalate (MCHT); 2×2×2 supercells are shown. The structures of the individual molecules are shown on the right. The radial distribution functions *g*(r) for the polymorphs in 3×3×3 supercells are shown in between. A Lorentzian broadening of 0.1 is used for smoothing the crystalline delta functions at the peak positions.

form intramolecular O–H···Cl bonds instead. The carboxymethyl groups are arranged almost perpendicular to the aromatic plane, which facilitates intermolecular O–H···O hydrogen bonds between the hydroxyl groups and the carboxymethyl groups due to π-stacked intermolecular arrangements. Grant and co-workers have studied the differences in the hydrogen-bonding patterns in the crystals by solid-state ^{13}C NMR spectroscopy, which unambiguously characterized the intramolecular O–H···O hydrogen bonds in the Y form and intramolecular O–H···Cl and intermolecular O–H···O hydrogen bonds in the W form.[14] Alsenoy and co-workers have performed calculations for supermolecule clusters with one monomer being surrounded by few nearest-neighbor molecules, which are further surrounded by point charges using the Hartree–Fock multiplicative integral approximation method. Calculations have revealed a small amount of charge-transfer interaction between the monomers (≈0.03 *e*) and substantially stronger intramolecular O–H···O hydrogen bonds compared to the intermolecular ones for the Y form.[15a] For the LY form, the intermolecular and intramolecular O–H···O hydrogen bonds are of almost equivalent strengths.[15b] Curtin et al. have shown that in the solution phase, the Y form and the W form are in a solvent-dependent equilibrium with a hybrid intermediate (H form) for which one –OH group has an intramolecular hydrogen bond to the carboxymethyl group and one to the Cl atom.[16]

Herein, based on a series of solid-state dispersion-corrected DFT calculations, we provide a detailed understanding of the relative stabilities of the W, LY, and Y polymorphs. We also provide a rationale for the lack of existence of the H form in the crystalline state. The origin of different colors in the polymorphs is traced to the conformations of the carboxymethyl groups relative to the aromatic plane and the nature of the O–H···O and O–H···Cl hydrogen bonds. The individual molecules are stabilized in the crystal through intermolecular π-stacking and H-bonding interactions wherein dispersion forces are shown to be a major component. The minimum-energy path for conversion of the global minimal crystalline form (Y) to the W form is found to be via the H form through sequential disrotatory out-of-plane motion of the two O–H bonds. A concerted motion of the two O–H bonds to lead to the W form via the LY form is found to be of higher energy.

Computational Methods

Dimethyl-3,6-dichloro-2,5-dihydroxyterephthalate (MCHT) has 26 atoms and the crystals of the Y and LY forms have 26 atoms in their unit cell. For the W form, the unit cell is dimerized with 52 atoms in its unit cell. For modeling both the ground state and absorption properties, DFT was a method of choice as wave-function-based methods were too expensive. We used both a localized Gaussian basis as well as the plane-wave-based DFT methods. Within the Gaussian basis, a split basis of 6-31G/Auto was used wherein the density fitting was generated automatically from the atomic orbital primitives for computing the Coulomb interactions.[17] We used the screened exchange in HSEh1PBE, a pure functional for calculations of the molecules as well as the crystals within the Gaussian basis.[18] Calculations at the popular B3LYP hybrid functional[19] level were also performed to verify the suitability of the pure exchange-based HSEh1PBE method in our systems, as the lack of proper long- and middle-range exchanges for the B3LYP method is well known.[20] All the calculations within the localized basis were performed using the Gaussian 09 suite of programs.[21] Modeling of the crystals was performed using the PWSCF (plane-wave self-consistent field) code within the generalized gradient approximation (GGA) and Perdew–Burke–Ernzerhof (PBE) functional as implemented in the Quantum Espresso Package.[22] The plane-wave basis set of 0.01 Ry Marzari–Vanderbilt smearing was used to describe valence electrons with a kinetic energy cutoff up to 30 Ry. Ionic cores were described by the ultrasoft pseudopotential.[23] The inputs for the crystal structures were generated from the experimental crystallographic information files (CIFs) of the Y, LY, and W forms.[24] All the atoms were allowed to relax. A 6×6×6 *k*-point mesh was used. The monomers were optimized by embedding the molecules within a cubical box with lattice constant = 20 Å. Dispersion interactions were consid-

ered using Grimme's DFT-D2 empirical formalism.[25] The stabilization energies for the crystals were calculated as $\Delta E = E_{crystal} - E_{monomer}$. The unit cell of the W crystal has twice the number of atoms as that of the molecule, so $E_{crystal}$ in W was divided by a factor of 2. Scans for the potential energy surfaces performed for transformation between the various intramolecular conformations were performed by disrotatory motion of the two –OH groups in both a sequential and simultaneous manner. All other structural parameters were optimized during the dihedral twist of the O–H group from the aromatic plane.

Results and Discussion

Figure 1 shows the optimized crystal structures of the Y, LY, H, and W polymorphs along with the structures of the molecules. The initial coordinates for the crystal optimization were retrieved from the CIFs of the Y, LY, and W forms. The unit cells contract by only about 4–6% with respect to the input CIFs. For generating the initial input for the crystal of the H form, the dihedral angle of one of the –OH groups along the aromatic plane of the molecule within the Y form was twisted by 180°. Apart from the diversity of packing of the molecules, the structures of the individual molecules show substantial differences. In the case of the Y form, the carboxymethyl groups are almost in the plane of the molecule whereas for the LY and W forms, they are rotated away from planarity. For the H form, the carboxymethyl group that is in intramolecular hydrogen bonding with the O–H bond is in plane, whereas the non-hydrogen-bonded one is out of plane to the aromatic ring. The O–H···O intramolecular hydrogen bond becomes longer (and therefore weaker) from 1.57 to 1.77 Å for Y→LY and Y→H. Further rotation of the carboxymethyl groups orients them perpendicular to the aromatic plane, thereby negating any remote possibility of an intramolecular O–H···O bond in the W form. Therefore, the two O–H bonds get themselves accommodated within the rather longer (and expectedly weaker) O–H···Cl intramolecular hydrogen bonds of length 2.72 Å. The relative stabilities among the crystals and the monomers in the four different conformations within the polymorphs are shown in Table 1. The structures of the individual molecules were retrieved from the crystals and only the hydrogen atoms were optimized.

As seen from Table 1, both the Gaussian basis set calculations and the plane-wave DFT-D2 calculations led to similar relative energies ($\approx$1 kcal mol^{-1}) for the Y and the LY polymorphs. The W polymorph is less stable according to our calculations. This is in nice agreement with the experimental observation

Table 1. Relative energies [kcal mol^{-1}] of the fully optimized crystals and their monomeric units (hydrogen atom optimized only).

Form	Crystal relative energies		Monomer relative energies	
	HSEh1PBE/ 6-31G/Auto	Plane wave (DFT-D2)	HSEh1PBE/ 6-31G/Auto	Plane wave (DFT-D2)
Y	0.7	0.0	0.0	0.0
LY	0.0	0.8	5.1	2.3
W	2.9	1.6	14.0	7.6
H	8.1	14.3	5.6	0.5

that at room temperature, the Y and LY forms are stable whereas the W form is stabilized at $T > 360$ K with an endothermicity (ΔH) of 0.6 kcal mol^{-1} (based on differential scanning calorimetric measurements) for the conversion from the Y to W form.[26] The H crystal is destabilized to such an extent that such a crystal structure is rather unlikely to exist. This again corroborates with the fact that the H form has been shown to exist only in the solution phase.[16]

For the monomers, the most stable conformation of the molecule exists in the case of the Y form, which becomes gradually unstable as the carboxymethyl group rotates out of the plane to lead to the LY/H form and finally to the W form, in which the two strong O–H···O hydrogen bonds are replaced by two weak O–H···Cl bonds. The stability of the monomers follows the trend: Y > LY ~ H > W. Although the relative order of stability is consistent for both the methods, the plane-wave DFT-D2 results are seen to underestimate the relative energies by almost 50%. The results are similar for comparison of the plane-wave DFT-D2 method with other localized Gaussian basis-based DFT methods such as B3LYP and M06-2X (see the Supporting Information). In our opinion, localized Gaussian basis calculations are more realistic descriptors of isolated molecules than the plane-wave-based methods. However, as estimation of the relative crystal stabilization energies for the plane-wave method rely on the relative energies between the different polymorphs and their respective isolated molecular units placed within a unit cell of large dimension, the underestimation gets cancelled out.

Interestingly, although the monomers are strongly destabilized in the W form, the W crystal is only marginally ($\approx$2–3 kcal mol^{-1}) less stable than the Y form in which the monomer is in its most stable conformation. Therefore, one might expect that intermolecular forces among the monomers in the W form in the crystal are strong enough to compensate for the lower stability in its conformation. To test this postulate, 3×3×3 supercells for each polymorph are considered to calculate the radial distribution functions, $g(r)$.[27] We maintain a center of distance of 12 Å as a cutoff. As seen from the radial distribution functions in Figure 1, for the Y, LY, and W polymorphs the most significant contribution arises from dimers with contact distance approximately 4 Å between the monomers. The case for the H form is remarkably different, as the significantly contributing dimers consist of monomers that are separated by as much as 6 Å. For all the crystals, these dimers have a slipped parallel π-stacked arrangement of the monomers. For the Y, LY, W, and H forms, in the slipped parallel π-stacked form, $d_{center\text{-}to\text{-}center}$ = 4.30, 3.93, 3.92, and 6.16 Å, respectively. To understand the stability associated with these arrangements, potential energy surfaces (PESs) were analyzed for variation in the center-to-center distances in these molecular arrangements. Calculations were performed at different DFT levels, namely B3LYP and M06-2X[28] apart from the HSEh1PBE and the plane-wave DFT-D2 method, to assess their performance for weak intermolecular interactions, particularly the dispersion forces, which are known to be important in supramolecular processes.[29] Figure 2 shows the PESs for all the π-stacked systems as the stabilization gained at the equilibrium distances are maximum

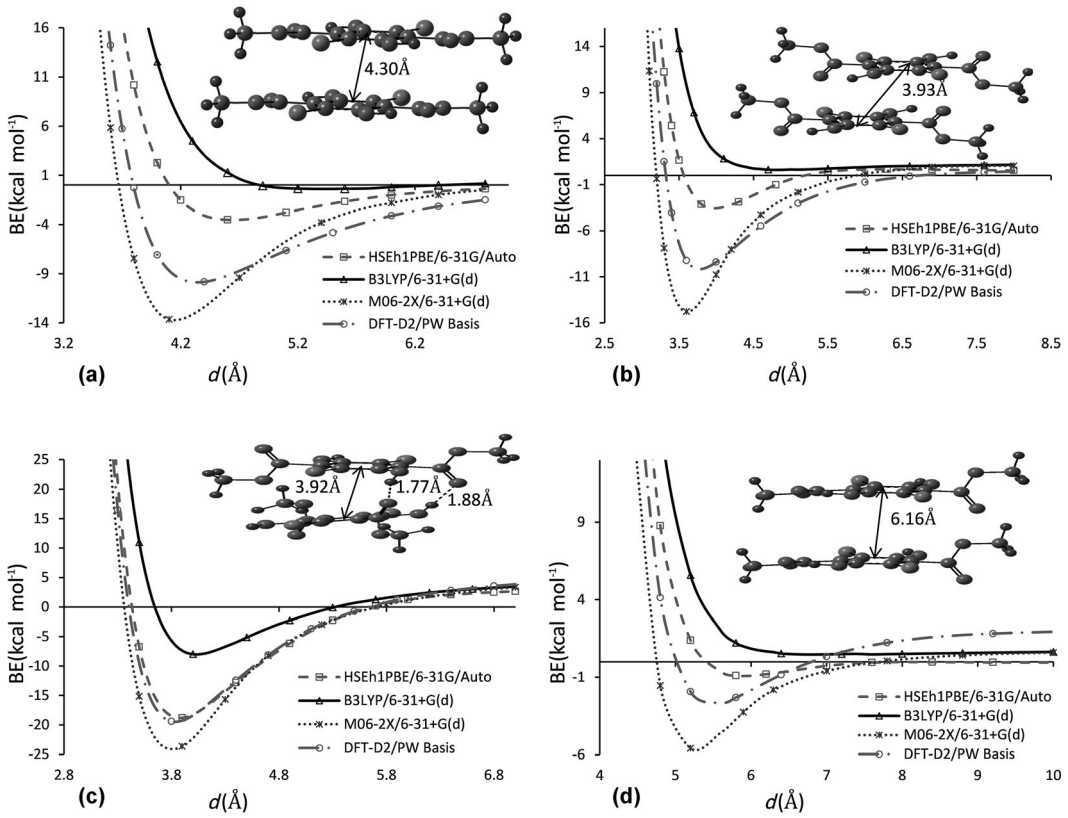

Figure 2. Potential energy surfaces for binding for the center-to-center displacements of the π-stacked dimers of a) yellow, b) light yellow, c) white, and d) hybrid crystals of MCHT at various levels of theory. BE = binding energy.

for them (the plots for the PESs for the linearly arranged dimers are shown in the Supporting Information). The performance of the B3LYP functional is rather poor, as for all the systems other than the stacked configuration in the W polymorph in Figure 2c it exhibits only a metastable dimer. Both the M06-2X and the DFT-D2 plane-wave methods, in which dispersion interactions are implicitly and explicitly included, respectively, show high binding energies at the equilibrium configurations. In our opinion, the M06-2X functional seems to show overbinding because for the π-stacked configuration in the H form (Figure 2d), at a distance of about 5.2 Å, it shows a binding energy of -6.0 kcal mol^{-1}, which is too high for such a large separation. Therefore, although the B3LYP method shows underbinding, the M06-2X method overbinds. Hence, in comparison, the performance of the HSEh1PBE is found to be quite good as it leads to binding energies that are almost exactly in between those predicted by the B3LYP and M06-2X methods. Also, the predicted equilibrium distances from PESs of the dimers at the HSEh1PBE level are similar to those obtained from their optimized crystal structures.

Nevertheless, the PES in Figure 2c predicts highest binding energies for the π-stacked dimer in the W form relative to the Y, LY, and H forms irrespective of the method of calculation. Curiously, though the center-to-center distances for the stacked dimers for the LY and W forms (shown in Figure 2b and Figure 2c, respectively) are almost the same, their PESs are remarkably different. Not only are stacked dimers for the W form more strongly bound, unlike the LY form, but also the PES for the W form is bound even at the B3LYP level. This is interesting as it has been shown previously that the B3LYP functional is incapable of reproducing a stable π-stacked dimer for aromatic systems.[30] Hence, if the stacked dimers in the W form were stabilized only through aromatic π–π interactions, one would have expected that the PES at the B3LYP level would lack a minimum (similar to that for the LY form in Figure 2b). A closer analysis of the structures of the stacked dimers shows that in the W form there are two additional intermolecular O–H···O hydrogen bonds of $d = 1.77$ and 1.88 Å. Such interactions are clearly lacking for the stacked dimers of the LY form. To quantitatively estimate the additional stabilization bestowed on the stacked dimer in the W form through intermolecular hydrogen bonds, the dihedral angles associated with the two O–H···O intermolecular hydrogen bonds were twisted at the HSEh1PBE/6-31G/Auto level. The modes of twisting along with the potential energy profiles for the scans are shown in the Supporting Information. From the difference in energies between the peak and the valley of the PES, the binding energies for the two hydrogen bonds are calculated as -5.0 kcal mol^{-1} (d(O–H···O) = 1.77 Å) and -5.0 kcal mol^{-1} (d(O–H···O) = 1.88 Å). At the HSEh1PBE/6-31G/Auto level, the calculated total binding energy for the stacked dimer from Figure 2c is -18.8 kcal mol^{-1}. Subtracting the contribution of the two intermolecular

hydrogen bonds from this, we estimate the π-stacking binding energy in the W form as −8.8 kcal mol^{-1}, which is a reasonable estimate for π-interacting substituted aromatic rings.[31]

To understand the pathways for transformation between the various forms, namely the Y, H, LY, and W structures, we calculated the minimum-energy pathways for the conversion. There are two possibilities for undergoing this: 1) stepwise, disrotatory, and out-of-plane rotation of the two –OH dihedral angles with respect to the aromatic plane, which breaks the two intramolecular O–H···O bonds and subsequently forms the two intramolecular O–H···Cl bonds; and 2) similar rotations in the –OH dihedral angles, simultaneously. Figure 3 shows the PESs

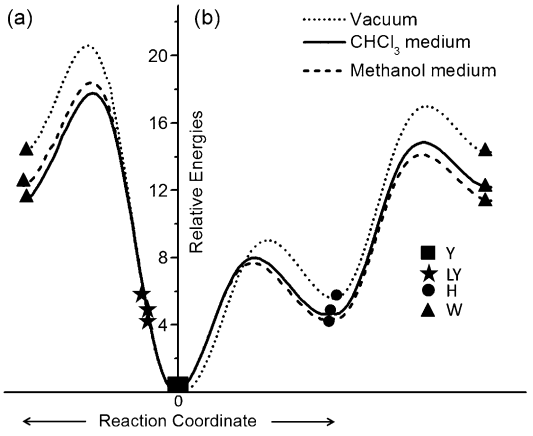

Figure 3. Potential energy surfaces [kcal mol^{-1}] in the gas phase, chloroform, and methanol for a) concerted and b) stepwise transformation of the W, LY, and H polymorphs from the Y form at the HSEh1PBE/6-31G/Auto level of theory.

for both possibilities. Importantly, all four polymorphs cannot be realized within in a single PES. For example, although the transformation of the W form from the global minimal Y form can be realized through both pathways, albeit with different barriers (discussed later), the H form can be formed from the Y form only through the stepwise disrotatory rotation of the –OH bonds. Similarly, the LY form can be realized from the Y form through concerted disrotatory rotation of the –OH bonds only.

Concerted disrotatory rotation of the two –OH dihedral angles is calculated to have a single barrier of $\Delta G^{\neq} = 20.6$ kcal mol^{-1} whereas the stepwise mechanism has two barriers of $\Delta G_1^{\neq} = 9.1$ and $\Delta G_2^{\neq} = 17.0$ kcal mol^{-1}. Although the barrier height for the concerted transformation is reduced by 2.2 and 2.8 kcal mol^{-1} in the methanol and chloroform solvent phases (within the polarizable continuum model, IEFPCM),[32] respectively, it is greater than that for the stepwise mechanism in solution. Clearly, a concerted pathway is of much higher energy and a transformation of the Y→W form is rather unlikely based on this mechanism. Nevertheless, the LY form exists on the concerted pathway as a relatively higher energy conformation (see Figure 3a).

The H form is an intermediate on the stepwise pathway and is realized through rotation of the first –OH dihedral angle from the Y form via transition state 1 (TS1), in which the –OH bond is perpendicular to the aromatic plane (see Figure 3b). Subsequent rotation of the second –OH bond in a disrotatory fashion with respect to the first –OH rotation from the H form leads to the H→W transformation via TS2, in which the second –OH bond is perpendicular to the aromatic plane. Increasing the dielectric constant of the solvent from a nonprotic medium (chloroform, $\varepsilon = 4.81$) and subsequently to a protic and H-bonding medium (methanol, $\varepsilon = 32.7$) leads to stabilization of TS1 and TS2 by 1.1 (1.4) and 2.2 (2.9) kcal mol^{-1} for chloroform (methanol), respectively, with respect to the gas phase. Notably, although an increase in the dielectric constant of the solvent also stabilizes the intermediate (H form) and the product (W form), the stabilization of the transition-state structures is relatively much more, as a polar medium is capable of solvating the free –OH bonds in the transition state in which neither the intramolecular O–H···O bond exists nor the intramolecular O–H···Cl bond is formed. Our calculations do indeed support and explain the molecular mechanism for the previous experiments by Curtin et al. in which a solvent-dependent equilibrium of the type Y⇌H⇌W was reported.[16] Nevertheless, based on the potential energy scans of the monomers (in the gas phase and solution), a direct correlation cannot be drawn to the solid-state transformations within the crystals.

Time-dependent DFT (TD-DFT) calculations[33] at the HSEh1PBE/6-31G/Auto level were performed on the hydrogen optimized structures of the monomers as retrieved from the crystals of the Y, LY, and W polymorphs. The monomer for the H form was retrieved from the optimized crystal structure of the H polymorph. Figure 4 shows the computed absorption spectra for the monomers in the gas phase for all four conformations. The transitions for the Y, LY, H, and W monomers were observed at 400.53 nm ($f = 0.1322$, HOMO→LUMO transition, 100%), 347.45 nm ($f = 0.1064$, HOMO→LUMO transition, 97.4%; HOMO−1→LUMO+2, 2.6%), 337.76 nm ($f = 0.1357$, HOMO→LUMO transition, 100%), and 272.76 nm ($f = 0.1213$,

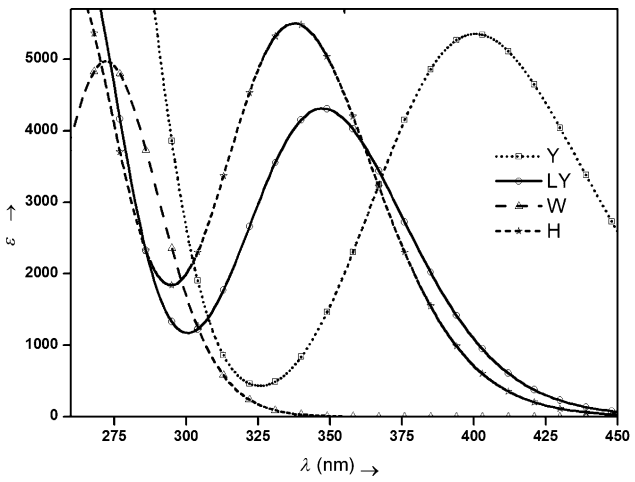

Figure 4. Computed absorption spectra for the monomers of the a) yellow, b) light yellow, c) white, and d) hybrid crystals of MCHT at the HSEh1PBE/6-31G/Auto level of theory.

HOMO→LUMO transition, 94.3%; HOMO−1→LUMO+1, 5.7%), respectively. Out of the four conformations, the calculated spectrum for the Y monomer is redshifted to the maximum extent absorbing in the visible violet region (400–450 nm), thereby imparting a yellow color as observed experimentally both for the crystal and in solution (see the Supporting Information for TD-DFT calculations in $CHCl_3$ and methanol media for the four conformers). The W monomer is calculated to absorb in the UV region. This is also in very good agreement with the colorless nature of the W crystal in the solution phase. For the LY and H monomers, the computed spectra are blueshifted by about 50–60 nm with respect to the Y form, which explains the pale yellow color for the LY form (in the crystal and in solution) and for the H form (in solution). Curtin and Byrn have reported that solvent polarity shifts the absorption maximum of MCHT from 400 nm in $CHCl_3$ to 356 nm in chloroform/ethanol mixture, and to 315 nm in ethanol. As the Y and W forms are stable in $CHCl_3$ and ethanol, respectively, the absorption at 315 nm was assigned to the W form, 356 nm to the H form, and 400 nm to the Y form, which is supported by our calculations on the MCHT monomers[16] (see the Supporting Information). TD-DFT calculations for the linear head-to-tail and the π-stacked dimers led to very little Davydov splitting with respect to the monomers (see the Supporting Information), thus resulting in only weak exciton coupling within the molecular aggregates.[34] Therefore, the absorption properties and hence the color in these polymorphic crystals are mostly governed by the individual molecular absorption. Based on the TD-DFT calculations, we find that an intramolecular O–H···O hydrogen bond leads to a bathochromic shift for the MCHT polymorph (maximum for Y, since it has two such interactions) whereas an intramolecular O–H···Cl bond leads a hypsochromic shift (maximum for W with two such interactions). The H form has one intramolecular O–H···O and one O–H···Cl bond, so the color is expectedly in between that of the Y and W forms, as observed. The case for the LY form is also somewhat similar as, even though it has no intramolecular O–H···Cl hydrogen bonds, the O–H···O bonds are substantially twisted (by $\approx 25^\circ$ with respect to the Y molecule, see Figure 1), which leads to only weak intramolecular O–H···O bonding. This, therefore, again leads to a hypsochromic absorption relative to the Y form.

Conclusion

The existence of various colors in crystals of 2,5-dihydroxyterephthalic acid and its 3,6-dihalo derivatives has been known for over 100 years. Although it is rather straightforward to expect a correlation between the structural aspects of these conformationally flexible molecules and their optical absorption, herein a one-to-one relationship is demonstrated. We show that two strong intramolecular O–H···O hydrogen bonds in the case of the Y polymorph ensure planarity of the molecules and bestow the characteristic yellow color both in the solid state and in solution. Weakening of the O–H···O bonds in the LY/H polymorphs leads to a blueshifted absorption (light yellow color), and their subsequent cleavage in the W form results in absorption only in the UV region and its experimentally observed white color. The contribution of the intramolecular O–H···Cl hydrogen bonds in the H and W forms to their optical absorption is found to be benign.

The present calculations also conclude that although the Y crystal is the most stable phase, the LY and W polymorphs are quite close in energy. This rationalizes the existence of all three phases under various experimental conditions. We also found a relatively higher energy polymorph, namely the H form, which has one intramolecular O–H···O and one O–H···Cl hydrogen bond. This form is shown to be an intermediate in the pathway for Y→W transformation. Synthesis of such a molecule within a crystal has not been accomplished to date, which we believe is primarily due to the lack of any reasonably strong intermolecular interactions (the aromatic rings are at a distance of ≈ 6 Å in the computed crystal structure, as shown in Figure 1). Though the possibility of weak intermolecular interactions among the molecules in the H form through C–H (methyl group)···O=C (carboxyl group) forces cannot be rejected, they are expected to be substantially fluxional to lead to thermal disorder and hamper single-crystal diffraction. Nevertheless, recent progress by Fujita and co-workers[35] to determine structures of noncrystalline molecules by absorbing (soaking) them in porous network complexes ("crystalline sponges") can be an excellent tool to isolate and determine the structure of the H form of MCHT. Measuring the energy changes associated with the Y→H→W transformation within the crystalline sponge by calorimetry could be an experimental strategy to verify our prediction.

Acknowledgements

A.D. and S.M.P. thank CSIR India for financial assistance. A.D. thanks DST, CSIR, and INSA for partial funding.

Keywords: density functional calculations · hydrogen bonds · molecular packing · polymorphism · solid-state structures

[1] a) N. Ruangsupapichat, M. P. Pollard, S. R. Harutyunyan, B. L. Feringa, *Nat. Chem.* **2011**, *3*, 53–60; b) J. Wang, L. Hou, W. R. Browne, B. L. Feringa, *J. Am. Chem. Soc.* **2011**, *133*, 8162–8164.

[2] a) J. Michl, C. H. Sykes, *ACS Nano* **2009**, *3*, 1042–1048; b) G. S. Kottas, L. I. Clarke, D. Horinek, J. Michl, *Chem. Rev.* **2005**, *105*, 1281–1376 and references therein.

[3] D. Jose, A. Datta, *J. Phys. Chem. Lett.* **2010**, *1*, 1363–1366.

[4] M. Furch, S. Fujita-Becker, M. A. Geeves, K. C. Holmes, D. Manstein, *J. Mol. Biol.* **1999**, *290*, 797.

[5] F. Nagatsugi, Y. Takahashi, M. Kobayashi, S. Kuwahara, S. Kusano, T. Chikuni, S. Hagihara, N. Harada, *Mol. BioSyst.* **2013**, *9*, 969–973.

[6] G. H. Koenderink, Z. Dogic, F. Nakamura, P. M. Bendix, F. C. MacKintosh, J. H. Hartwig, T. P. Stossel, D. A. Weitz, *Proc. Natl. Acad. Sci. USA* **2009**, *106*, 15192–15197.

[7] a) H. L. Tierney, C. J. Murphy, A. D. Jewell, A. E. Baber, E. V. Iski, H. Y. Khodaverdian, A. F. McGuire, N. Klebanov, C. H. Skkes, *Nat. Nanotechnol.* **2011**, *6*, 625–629; b) B. K. Pathem, S. A. Claridge, Y. B. Zheng, P. S. Wiess, *Annu. Rev. Phys. Chem.* **2013**, *64*, 605–630 and references therein.

[8] a) Y. L. Slovokhotov, I. S. Neretin, J. A. K. Howard, *J. New Chem.* **2004**, *28*, 967–979; b) A. Datta, S. K. Pati, D. Davis, K. Sreekumar, *J. Phys. Chem. A* **2005**, *109*, 4112–4117; c) D. M. Alloway, M. Hofmann, D. L. Smith, N. E.

Gruhn, A. L. Graham, R. Colorado, V. H. Wysocki, T. R. Lee, P. A. Lee, N. R. Armstrong, *J. Phys. Chem. B* **2003**, *107*, 11690 – 11699.
[9] M. K. Mishra, S. Varughese, U. Ramamurthy, G. R. Desiraju, *J. Am. Chem. Soc.* **2013**, *135*, 8121.
[10] a) G. R. Desiraju, *J. Am. Chem. Soc.* **2013**, *135*, 9952; b) A. Y. Lee, D. Erdemir, A. S. Myerson, *Annu. Rev. Chem. Biomol. Eng.* **2011**, *2*, 259 – 280; c) J. D. Dunitz, J. Bernstein, *Acc. Chem. Res.* **1995**, *28*, 193 – 200.
[11] L. Yu, *Acc. Chem. Res.* **2010**, *43*, 1257 – 1266.
[12] a) A. Hantzsch, *Chem. Ber.* **1915**, *48*, 797; b) A. Hantzsch, *Chem. Ber.* **1915**, *48*, 785.
[13] J. Swiatkiewicz, P. N. Prasad, *J. Am. Chem. Soc.* **1982**, *104*, 6913 – 6918.
[14] M. Strohmeier, A. M. Orendt, D. W. Alderman, D. M. Grant, *J. Am. Chem. Soc.* **2001**, *123*, 1713 – 1722.
[15] a) A. Peeters, A. T. H. Lenstra, E. Van Doren, C. Van Alsenoy, *J. Mol. Struct.: THEOCHEM* **2001**, *546*, 25 – 32; b) A. Peeters, A. T. H. Lenstra, E. Van Doren, C. Van Alsenoy, *J. Mol. Struct.: THEOCHEM* **2001**, *546*, 17 – 24.
[16] D. Y. Curtin, S. R. Byrn, *J. Am. Chem. Soc.* **1969**, *91*, 6102 – 6106.
[17] B. I. Dunlap, *J. Chem. Phys.* **1983**, *78*, 3140 – 3142.
[18] J. Heyd, G. E. Scuseria, M. Ernzerhof, *J. Chem. Phys.* **2006**, *124*, 219906.
[19] A. D. Becke, *J. Chem. Phys.* **1993**, *98*, 5648 – 5652.
[20] See D. Jose, A. Datta, *Cryst. Growth Des.* **2011**, *11*, 3137 as a representative example.
[21] Gaussian 09, Revision A.01, M. J. Frisch, G. W. Trucks, H. B. Schlegel, G. E. Scuseria, M. A. Robb, J. R. Cheeseman, G. Scalmani, V. Barone, B. Mennucci, G. A. Petersson, H. Nakatsuji, M. Caricato, X. Li, H. P. Hratchian, A. F. Izmaylov, J. Bloino, G. Zheng, J. L. Sonnenberg, M. Hada, M. Ehara, K. Toyota, R. Fukuda, J. Hasegawa, M. Ishida, T. Nakajima, Y. Honda, O. Kitao, H. Nakai, T. Vreven, J. A. Montgomery, Jr., J. E. Peralta, F. Ogliaro, M. Bearpark, J. J. Heyd, E. Brothers, K. N. Kudin, V. N. Staroverov, R. Kobayashi, J. Normand, K. Raghavachari, A. Rendell, J. C. Burant, S. S. Iyengar, J. Tomasi, M. Cossi, N. Rega, J. M. Millam, M. Klene, J. E. Knox, J. B. Cross, V. Bakken, C. Adamo, J. Jaramillo, R. Gomperts, R. E. Stratmann, O. Yazyev, A. J. Austin, R. Cammi, C. Pomelli, J. W. Ochterski, R. L. Martin, K. Morokuma, V. G. Zakrzewski, G. A. Voth, P. Salvador, J. J. Dannenberg, S. Dapprich, A. D. Daniels, Ö. Farkas, J. B. Foresman, J. V. Ortiz, J. Cioslowski, D. J. Fox, Gaussian, Inc. Wallingford CT, **2009**.
[22] P. Giannozzi, S. Baroni, N. Bonini, M. Calandra, R. Car, C. Cavazzoni, D. Ceresoli, G. L. Chiarotti, M. Cococcioni, I. Dabo, A. Dal Corso, S. de Gironcoli, S. Fabris, G. Fratesi, R. Gebauer, U. Gerstmann, C. Gougoussis, A. Kokalj, M. Lazzeri, L. Martin-Samos, N. Marzari, F. Mauri, R. Mazzarello, S. Paolini, A. Pasquarello, L. Paulatto, C. Sbraccia, S. Scandolo, G. Sclauzero, A. P. Seitsonen, A. Smogunov, P. Umari, R. M. Wentzcovitch, *J. Phys. Condens. Matter* **2009**, *21*, 395502.
[23] The pseudopotentials used were from http://www.quantum-espresso.org.
[24] The CIFs were retrieved from the Cambridge Crystallographic Data Centre (CCDC), see F. H. Allen, *Acta Crystallogr. Sect. B* **2002**, *58*, 380 – 388.
[25] S. Grimme, *J. Comput. Chem.* **2006**, *27*, 1787.
[26] S. R. Byrn, D. Y. Curtin, I. C. Paul, *J. Am. Chem. Soc.* **1972**, *94*, 890 – 898.
[27] A. Datta, S. Mohakud, S. K. Pati, *J. Chem. Phys.* **2007**, *126*, 144710.
[28] Y. Zhao, D. G. Truhlar, *J. Chem. Phys.* **2006**, *125*, 194101.
[29] a) A. K. Jissy, U. M. P. Ashik, A. Datta, *J. Phys. Chem. C* **2011**, *115*, 12530; b) A. Nijamudheen, D. Jose, A. Shine, A. J. Datta, *J. Phys. Chem. Lett.* **2012**, *3*, 1493.
[30] M. O. Sinnokrot, E. F. Valeev, C. D. Sherrill, *J. Am. Chem. Soc.* **2002**, *124*, 10887 – 10893.
[31] M. O. Sinnokrot, C. D. Sherrill, *J. Phys. Chem. A* **2003**, *107*, 8377 – 8379.
[32] J. Tomasi, B. Mennucci, R. Cammi, *Chem. Rev.* **2005**, *105*, 2999 – 3093.
[33] R. Bauernschmitt, R. Ahlrichs, *Chem. Phys. Lett.* **1996**, *256*, 454 – 464.
[34] A. Datta, S. K. Pati, *Chem. Soc. Rev.* **2006**, *35*, 1305.
[35] Y. Inokuma, S. Yoshioka, J. Ariyoshi, T. Arai, Y. Hitora, k. Takada, K. Matsunaga, K. Rissanen, M. Fujita, *Nature* **2013**, *495*, 461 – 466.

Received: August 24, 2013
Revised: November 29, 2013
Published online on ■■ ■■, 0000

FULL PAPER

Polymorphism

*S. M. Pratik, A. Nijamudheen, S. Bhattacharya, A. Datta**

■■ – ■■

Color Polymorphism: Understanding the Diverse Solid-State Packing and Color in Dimethyl-3,6-dichloro-2,5-dihydroxyterephthalate

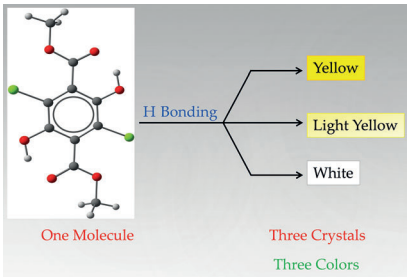

Multiple personality: A single chromophore exhibits three different colors depending on the nature of its packing in crystals (see figure) due to a tug-of-war among the intra- and intermolecular hydrogen bonds. Time-dependent DFT calculations reveal the role of the various types of hydrogen bonds in controlling the color of the polymorphs.